Journal of the Physical Society of Japan
Vol. 66, No. 2, February, 1997, pp. 493-498

Two-Phonon Assisted Indirect Exciton Luminescence in α-ZnP_2

Kaizo NAKAMURA*, Osamu ARIMOTO**, Masaru EGUCHI***
and Mitsuo NISHIKAWA****

Department of Physics, Faculty of Science, Okayama University, Okayama 700

(Received September 17, 1996)

Luminescence spectra of tetragonal ZnP_2 crystal are measured at various temperatures. Below the indirect exciton threshold, about 30 intrinsic indirect exciton luminescence bands are confirmed. Amidst the broad bound exciton luminescence band, several emission bands appear even at 2 K. Intensities of these bands increase with increasing temperature, especially in the high energy part of the band. They are also intrinsic exciton luminescence caused through the indirect exciton transition processes accompanied by two phonons at $\boldsymbol{k}_1$ and $\boldsymbol{k}_2$ conserving the exciton wavevector; $\boldsymbol{k}_{ex} = \boldsymbol{k}_1 + \boldsymbol{k}_2$. Energy difference between the lowest edges of one- and two-phonon luminescence bands 59.4 meV is equal to the largest Raman shift energy. Phonons participating in the luminescence are mainly momentum conserving phonons appearing in the one-phonon luminescence bands and the ones at the Γ point of the Brillouin zone.

KEYWORDS: ZnP_2, indirect exciton, luminescence, one-phonon process, two-phonon processes

§1. Introduction

Zinc diphosphide crystal ZnP_2 has two polymorphs: a red tetragonal form α-ZnP_2 and a black monoclinic form β-ZnP_2.[1,2] Optical properties of β-ZnP_2 have been investigated extensively,[3-5] including the magneto-optical measurement on the triplet exciton series.[6-8] Recently relaxation processes of exciton polariton have been studied in detail.[9-12] Nonlinear two photon absorption experiment gives deeper understanding of the electronic structure.[13]

Several works on the optical properties of the red ZnP_2 have been reported so far.[14-18] Energy gap of this material was said to be of indirect type. Rubenstein and Dean have measured luminescence spectra at 4.2 K and also reported that the indirect absorption edge was located at 2.216 eV. They have observed strong bound exciton luminescence accompanied by a very sharp zero phonon line BE^0 at 2.1445 eV followed by a broad phonon side band with much fine structure.[14] They have observed only the luminescence originated from defects. Several phonon energies deduced from the vibronic structure of the luminescence were given. Strong luminescence due to bound excitons has been reported in the cathode luminescence experiments, too.[15] Syrbu *et al.*[18] have reported the absorption edge with many steps for two polarizations. Also they observed many luminescence peaks immediately below the absorption edge. They have assigned some of these peaks as indirect exciton luminescence, and have related each luminescence peak to the corresponding absorption edge. Energy of the indirect exciton edge thus estimated was 2.208 eV, which coincides with the value in ref. 14.

The α-ZnP_2 crystal has 8 formula units in the tetragonal primitive unit cell. Therefore, we have utmost 72 modes of lattice vibration branches at the point of the indirect exciton bottom $\boldsymbol{k}_{ex}$ in the Brillouin zone which is not located yet. Several reports on Raman scattering[19-22] and infrared reflection spectra[23] are present. The number of luminescence bands corresponds to the number of phonon modes at the critical point $\boldsymbol{k}_{ex}$ which couple the exciton working as momentum conserving phonons.

In the present study, we have measured the absorption and luminescence spectra near the indirect absorption threshold. Raman spectra have been measured also at 2 K. Temperature change of the luminescence is investigated in detail to ascertain the intrinsic nature of the luminescence. If the luminescence is intrinsic, its spectral shape will be of Maxwellian distribution function reflecting the thermal population of the exciton. We have confirmed about 30 intrinsic exciton luminescence bands. These emission spectra will be compared with the Raman spectra which will afford some information about lattice vibrations, though the phonon frequencies obtained from the Raman spectra are those at the Γ point $\boldsymbol{k} = 0$ in the Brillouin zone. Low energy part of the luminescence has also been measured. Relation between the intrinsic exciton luminescence and the bound exciton luminescence is also found.

§2. Experimental Procedure

The starting materials were metallic zinc (99.999%) and red phosphorus (99.9999%) both from Furuuchi Chemicals. Single crystals of red zinc diphosphide were grown from vapor phase as the byproduct of β-ZnP_2.[4] The size of the specimen used for the optical measurement was $4 \times 4 \times 0.6$ mm ($a \times a \times c$). Surface of an as-grown crystal is perpendicular to the c-axis. Measure-

* E-mail: nakamura@psun.phys.okayama-u.ac.jp
** E-mail: arimoto@science.okayama-u.ac.jp
*** Present address: Asahi Optical Co., Ltd., Itabashi, Tokyo 174.
**** Present address: Toshiba Machine Co., Ltd., Chuo, Tokyo 104.

ment at 2 K was performed by immersing the specimen directly into the superfluid helium. For the experiments of temperature change, a continuous flow type cryostat (Oxford CF1204D) was employed. Absorption spectra was measured by using a tungsten lamp as a light source. For luminescence and Raman measurements, an argon laser (Spectra Physics 2017) and also a dye laser (Spectra Physics 375B) were used as exciting light sources. Light from the sample was analyzed through a double monochromator (Spex 1402) and a cooled photomultiplier (Hamamatsu R943-02). No correction was made for the sensitivity of the detecting system.

§3. Results and Discussion

3.1 One-phonon exciton luminescence

Figure 1 shows the luminescence spectrum of α-ZnP_2 at 2 K. Excitation was made by illuminating the crystal with the 514.5 nm line of Ar laser. At 2.14 eV, a very sharp line is seen. This line is the zero phonon line BE^0 of the bound exciton luminescence[14] followed by the weak and broad luminescence band extending to below 2 eV which includes the phonon side band of the BE^0 line. Several emission lines which are not reported so far are also seen below the BE^0 line. To be noted here is that the bound exciton luminescence is weak even at 2 K. Above this BE^0 line, about 30 narrow emission bands are observed up to 2.2 eV with a main peak at 2.149 eV. The peak intensity of this main line is far stronger than that of the BE^0 line, quite different from the result in ref. 14, in which the BE^0 line is the strongest.

High energy part of Fig. 1 is shown in Fig. 2. Except the BE^0 line, these luminescence bands show asymmetric spectral shape and similar in shape with each other, i.e., very steep rise at low energy tail and rather gradual decrease towards high energy tail. Sharp peaks like a zero phonon line of bound exciton luminescence reported by Syrbu *et al.*[18] were not observed in this region. The characteristic spectral shape of these emission bands reminds us of the Maxwellian distribution function reflecting the density of states of a parabolic energy band with thermal distribution of the indirect excitons.

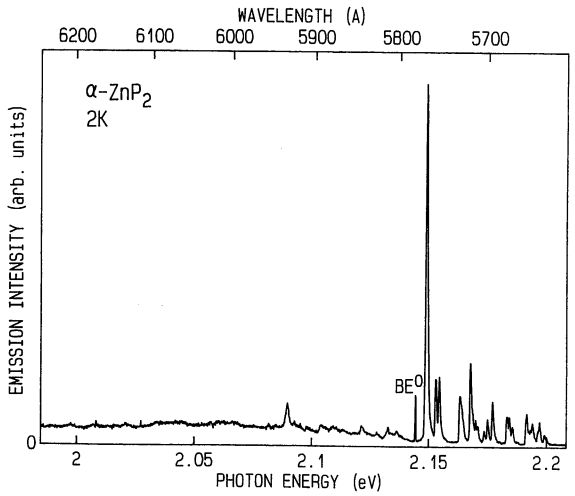

Fig. 1. Luminescence spectrum of α-ZnP_2 at 2 K. A sharp line BE^0 is the zero phonon line of the bound exciton luminescence.

Hence, temperature change gives us a definite evidence of the free exciton luminescence.

Figure 3 shows the temperature dependence of the spectral profiles of the luminescence for several temperatures. As the temperature is raised, the high energy side of each luminescence band broadens, keeping the low energy edge almost unchanged except the slight thermal broadening of the tail. To be noted here is that the zero phonon line of the bound exciton luminescence BE^0 decreases its intensity while its shape is almost unchanged. The change of spectral shape observed is just as we ex-

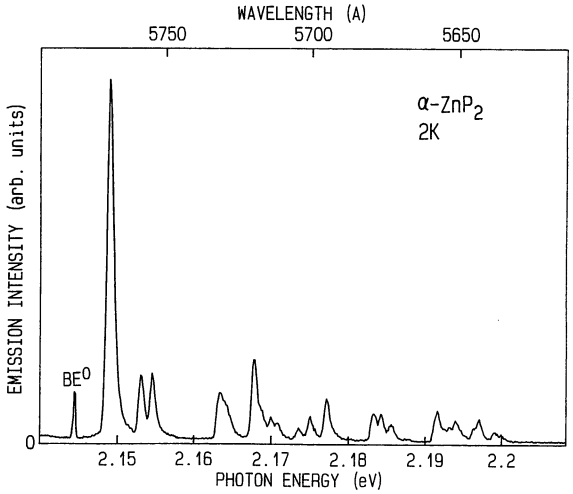

Fig. 2. High energy part of Fig. 1. Each luminescence band shows profile characteristic of Maxwellian function.

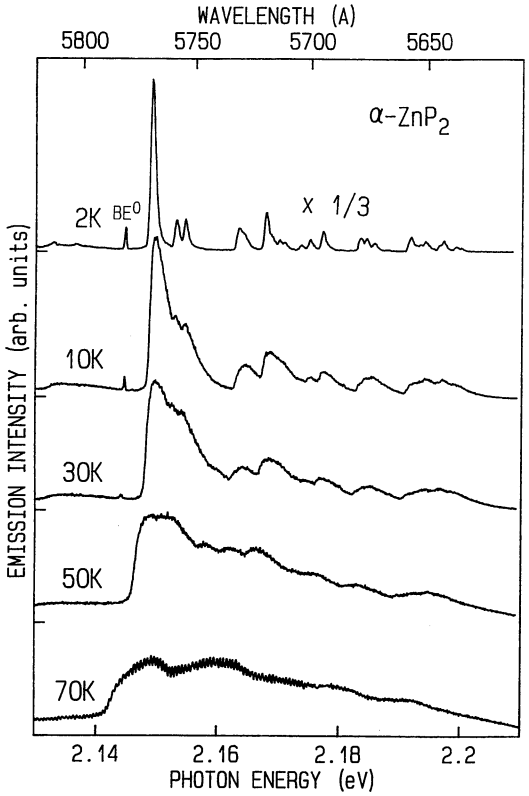

Fig. 3. Luminescence spectra of α-ZnP_2 at various temperatures. Measured temperature is shown in each spectrum.

pected for the Maxwellian distribution function. Therefore, the spectrum at 2 K in Fig. 2 is analyzed to get the threshold energy and the intensity of each member of luminescence bands composing the spectrum. We are, thus, able to resolve, *at least*, 30 components.

Absorption spectrum of α-ZnP_2 of thickness 0.6 mm was measured at 2 K. Incident light is parallel to the c-axis. Absorption increases gradually from 2.2 eV. From this spectrum, however, any distinct step-like structure of the indirect absorption edge was not confirmed owing to small thickness of the sample available. To distinguish the edge structure, we differentiate the absorption spectrum with energy, because the square root form of the absorption structure will give the sharp peak at the absorption edge when differentiated.[24] Several peaks were revealed as shown in Fig. 4 and some of these may correspond to the absorption edges. Comparing the luminescence spectrum in Fig. 2 with the derivative absorption spectrum in Fig. 4, a certain mirror symmetry is found among them. If we relate the low energy threshold of the strongest band at 2.148 eV with the derivative absorption peak at 2.268 eV, then we can estimate the indirect exciton energy $\hbar\omega_{ex}$ as 2.208 eV, in good agreement with reported values.[14,18] Together with threshold energies of luminescence bands thus obtained and the exciton energy $\hbar\omega_{ex}$, the energy of the momentum conserving phonon $\hbar\omega_i$ contributing to the i-th luminescence band is determined. Energies of momentum conserving phonons thus resolved and intensities of luminescence bands associated with them are summarized in Table I. The largest momentum conserving phonon energy obtained is 59.3 meV.

By using the indirect exciton energy $\hbar\omega_{ex} = 2.208$ eV and these phonon energies, we can calculate the spectral shape of luminescence at temperature T according as the following empirical formula,

$$I(\omega) = \frac{A}{\sqrt{k_B T}} \sum_{i=1}^{30} c_i(\omega_i(\boldsymbol{k}_{ex}))N_i(\omega_i(\boldsymbol{k}_{ex})) \times \sqrt{\omega - \omega_{oi}} \exp\left(-\frac{\hbar\omega - \hbar\omega_{oi}}{k_B T}\right)\theta(\omega - \omega_{oi}), \tag{3.1}$$

where $\hbar\omega$ is a photon energy, A a normalization constant, k_B the Boltzmann constant, c_i the coupling constant between the exciton and the i-th phonon, $\boldsymbol{k}_{ex}$ the wavevector at the bottom of the exciton band,

$$\omega_{oi} = \omega_{ex} - \omega_i(\boldsymbol{k}_{ex}), \tag{3.2}$$

$$N_i(\omega_i(\boldsymbol{k}_{ex})) = 1 + n_i(\omega_i(\boldsymbol{k}_{ex})) \tag{3.3}$$

for phonon emission, where

$$n_i(\omega_i) = \frac{1}{\exp\left(\frac{\hbar\omega_i}{k_B T}\right) - 1}, \tag{3.4}$$

and

$$\theta(\omega) = \begin{cases} 1 & \omega \geq 0 \\ 0 & \omega < 0. \end{cases} \tag{3.5}$$

Here $c_i N_i$ in eq. (3.1) represents the exciton-phonon coupling strength for the i-th momentum conserving phonon at $\boldsymbol{k}_{ex}$,[25] and is proportional to the intensity of the i-th component of the luminescence determined above. In the expression (3.1), the exciton band is assumed spherical, and the energy dependence of the c_i is ignored. For practical calculation, certain lifetime, or thermal broadening effect modifies eq. (3.1) a little.

For example, the result at $T = 30$ K is shown by a broken line in Fig. 5. The observed spectrum at 25 K is

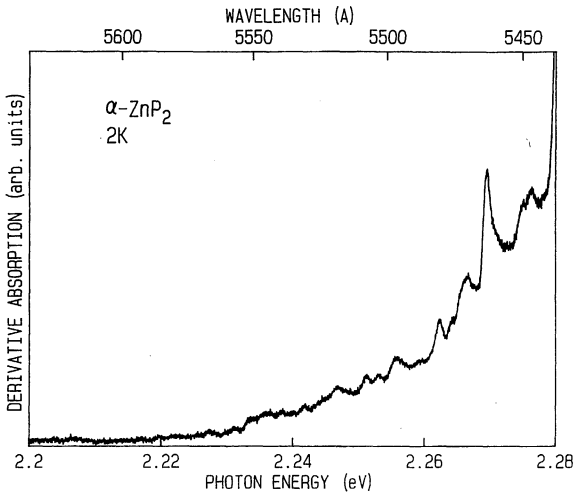

Fig. 4. Wavelength derivative of the absorption spectrum of α-ZnP_2 at 2 K. A prominent peak at 2.268 eV corresponds to the strongest luminescence peak at 2.149 eV.

Table I. Energies of momentum conserving phonons derived from the luminescence spectrum at 2 K, where $\hbar\omega_{ex} = 2.208$ eV is assumed. Integrated intensity for each luminescence band is also tabulated.

phonon energy (meV)	intensity
59.3	31.0
55.0	4.6
53.6	4.3
44.9	3.0
44.5	1.3
43.9	1.3
43.2	0.4
40.3	6.0
39.3	1.1
38.0	1.3
37.2	0.8
34.7	1.2
33.1	1.7
31.0	3.0
24.9	2.1
23.9	1.6
22.6	1.0
20.6	0.2
16.6	2.4
15.5	0.6
14.8	0.7
14.1	1.1
13.4	0.1
12.9	0.2
11.8	0.9
11.0	1.2
9.0	0.7
8.1	0.2

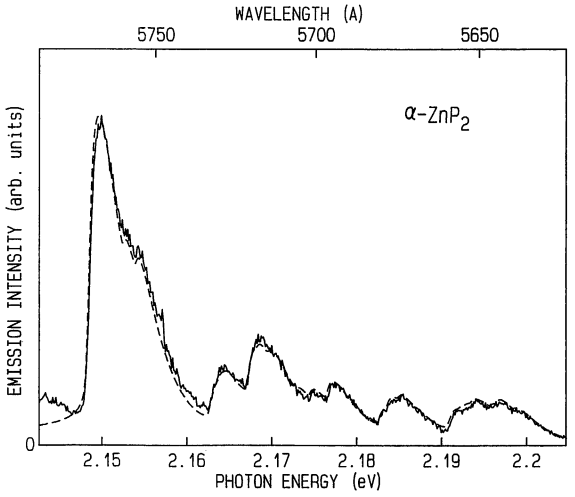

Fig. 5. Calculated luminescence spectrum of α-ZnP_2 at 30 K (broken curve) and observed spectrum at 25 K (solid curve).

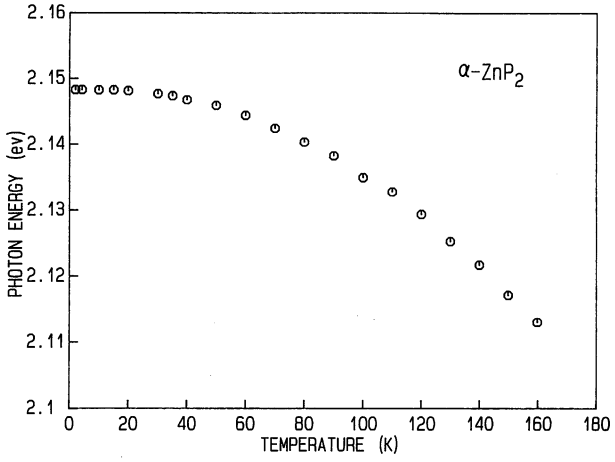

Fig. 6. Energy shift of the lowest edge of the strongest luminescence band in α-ZnP_2 with temperature.

also shown by a solid line. Excellent agreement was obtained over the whole region of the luminescence. For any spectrum, the temperature for the fitting is several degrees higher than the temperature of the sample holder. From these results, we conclude that these luminescence bands result from the intrinsic indirect exciton transition assisted by, at least, 30 momentum conserving phonons at the critical point $\boldsymbol{k}_{\rm ex}$ in the Brillouin zone.

In Fig. 6 is shown the energy shift of the lowest threshold of the exciton luminescence bands with the temperature. This displacement should be parallel to the energy shift of the indirect exciton threshold itself, if the energy of the momentum conserving phonon does not change over the temperature range observed.

3.2 Two-phonon exciton luminescence

Below the BE^0 line in Fig. 1, spectral shape is quite different from that in ref. 14. Many phonon lines reported by Rubenstein and Dean are not found in this spectrum. Several emission lines between 2.08 eV and the BE^0 line show characteristic shapes having rather steep edge at low energy side and tailing off to high energy side. Their spectral features are similar to the free exciton luminescence bands as described above, but the bandwidths are somewhat broad. Moreover, the separation ΔE between low energy thresholds of 2.09 eV band and 2.149 eV band is 59.4 meV, which is equal to the largest Raman shift energy and almost the same as the largest momentum conserving phonon energy.

As the temperature is raised, the high energy side of each luminescence band broadens, keeping the low energy edge almost unchanged as is seen in the free exciton luminescence described above. Temperature dependence of these emission bands is shown in Fig. 7. At higher temperatures where the broad bound exciton luminescence disappears, the luminescence survives. Especially, the growth is conspicuous in high energy region. Moreover the temperature shift of the lowest energy threshold is parallel to that shown in Fig. 6, where the separation ΔE between two thresholds is constant, 59.4 meV. From these facts, we conclude that these emission bands are free exciton recombination luminescence accompanied by two momentum conserving phonons, $\omega_i(\boldsymbol{k}_1)$ and $\omega_j(\boldsymbol{k}_2)$, which satisfy the following conservation condition,

$$\boldsymbol{k}_{\rm ex} = \boldsymbol{k}_1 + \boldsymbol{k}_2, \tag{3.6}$$

where $\boldsymbol{k}_1$ and $\boldsymbol{k}_2$ indicate wave vectors of phonons, and i and j their branches.

Intensity of each exciton transition is proportional to the product of two phonon numbers, and the resultant intensity at $\hbar\omega$ below the BE^0 peak is given as,

$$\begin{aligned} I_2(\omega) = \frac{B}{\sqrt{k_{\rm B}T}} \sum_{\boldsymbol{k}_1}\sum_{\boldsymbol{k}_2}\sum_{ij} & c_{ij}(\omega_i(\boldsymbol{k}_1)\omega_j(\boldsymbol{k}_2)) \\ & \times N_i(\omega_i(\boldsymbol{k}_1))N_j(\omega_j(\boldsymbol{k}_2)) \\ & \times \sqrt{\omega - \omega_{{\rm o}ij}} \exp\left(-\frac{\hbar\omega - \hbar\omega_{{\rm o}ij}}{k_{\rm B}T}\right) \\ & \times \theta(\omega - \omega_{{\rm o}ij})\delta(\boldsymbol{k}_1 + \boldsymbol{k}_2 - \boldsymbol{k}_{\rm ex}), \end{aligned} \tag{3.7}$$

where B is a normalization constant, the factor $c_{ij}N_iN_j$ represents the coupling strength[26] between the exciton and two phonons, $\omega_i(\boldsymbol{k}_1)$ and $\omega_j(\boldsymbol{k}_2)$, taking parts in the two-phonon transition,

$$N_i(\omega_i(\boldsymbol{k}_1)) = 1 + n_i(\omega_i(\boldsymbol{k}_1)) \tag{3.8}$$

for phonon emission,

$$\omega_{{\rm o}ij} = \omega_{\rm ex} - \omega_i(\boldsymbol{k}_1) - \omega_j(\boldsymbol{k}_2), \tag{3.9}$$

and $\boldsymbol{k}$'s run over whole Brillouin zone.

Then the equation (3.7) becomes,

$$\begin{aligned} I_2(\omega) = \frac{B}{\sqrt{k_{\rm B}T}} \sum_{\boldsymbol{k}}\sum_{ij} & c_{ij}(\omega_i(\boldsymbol{k})\omega_j(\boldsymbol{k}_{\rm ex} - \boldsymbol{k})) \\ & \times N_i(\omega_i(\boldsymbol{k}))N_j(\omega_j(\boldsymbol{k}_{\rm ex} - \boldsymbol{k})) \\ & \times \sqrt{\omega - \omega_{{\rm o}ij}} \exp\left(-\frac{\hbar\omega - \hbar\omega_{{\rm o}ij}}{k_{\rm B}T}\right) \\ & \times \theta(\omega - \omega_{{\rm o}ij}), \end{aligned} \tag{3.10}$$

where

$$\omega_{{\rm o}ij} = \omega_{\rm ex} - \omega_i(\boldsymbol{k}) - \omega_j(\boldsymbol{k}_{\rm ex} - \boldsymbol{k}). \tag{3.11}$$

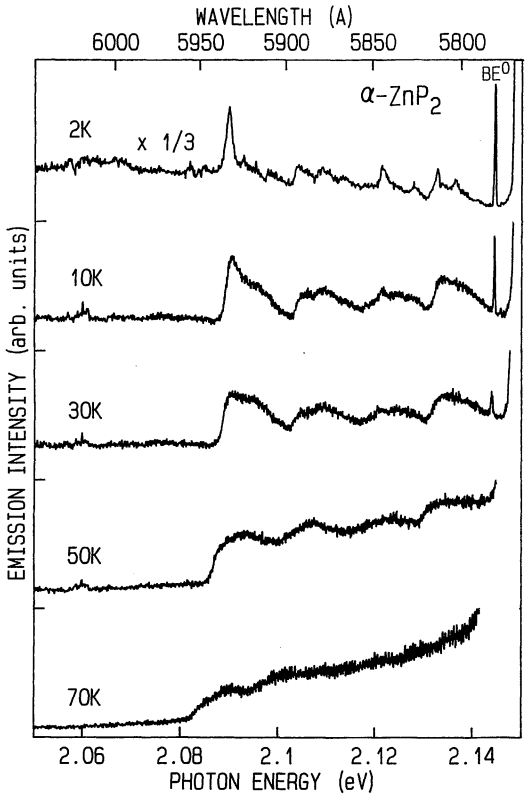

Fig. 7. Two-phonon assisted indirect exciton luminescence in α-ZnP_2 at various temperatures.

This model explains well the present results. Any combination of two phonons satisfying the condition (3.6) contributes to the luminescence according as the magnitude of the coupling strength. This spectral shape is a specially combined two-phonon density of states convoluted with Maxwellian distribution function of the indirect exciton. Therefore, the phonons at the critical point, where density of states is high, play important roles. Expected combined critical points are, for example, $\boldsymbol{k}_{ex}$ and $\boldsymbol{k}_\Gamma$ (=0). The separation ΔE described above is, therefore, $\hbar\omega_0(\boldsymbol{k}_\Gamma)$, the optical phonon energy at the center of the Brillouin zone, which should be compared with the Raman spectrum.

Figure 8 shows the Raman spectrum of α-ZnP_2 at 2 K. Many scattering lines appear between 5 and 60 meV. Our result is consistent with the previous reports.[19-22] The largest Raman shift energy is 59.4 meV. This energy is just the value ΔE. By comparing Fig. 8 with the luminescence spectrum Fig. 1 at 2 K, we find that several energy separations between the low energy edge of a one-phonon band and the one of a two-phonon band coincide with some of Raman shift energies. If we assume the coupled phonons for the lowest edge of two-phonon band to be on the same branch, then the dispersion of this branch is very small.

At higher temperatures, distribution of low energy phonons increases more than that of high energy ones. Hence the effect results in the growth of luminescence intensity in the high energy part of the two-phonon region. This tendency is more conspicuous in two-phonon luminescence than in one-phonon luminescence. In the one-phonon region, where we have defined tacitly, two-phonon luminescence components are also present. As a matter of fact, addition of small energy phonons and, at high temperatures, both phonon emission and absorption processes contribute to the two-phonon luminescence intensity in the one-phonon region. But the behavior is too complex to separate the two-phonon components from the one-phonon components.

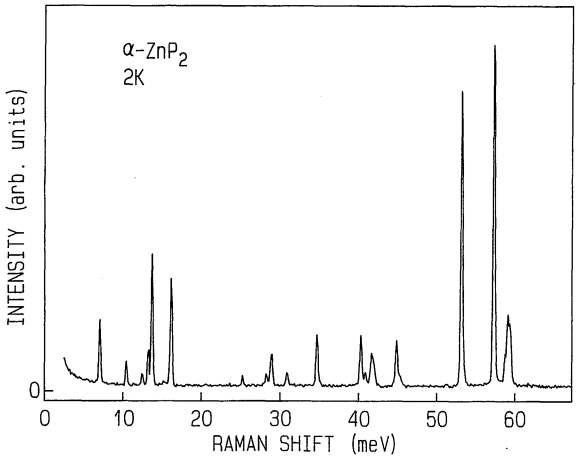

Fig. 8. Raman spectrum of α-ZnP_2 at 2 K.

Two-phonon assisted indirect exciton luminescence have been reported in several crystals, for example, diamond at high temperatures,[27] and Si.[28,29] In this experiment, however, change of the spectral profile of the one-phonon and also the two-phonon luminescence are investigated in detail with the change of temperature.

As described above, the bound exciton luminescence[14] is weak in this experiment. Therefore we have been able to observe the two-phonon luminescence even at 2 K. This seems to indicate that the purity of the crystal is very high. This fact also allows us detailed investigation of the relaxation processes in β-ZnP_2.[4,5,9,11,12]

Contrary to the present result, when the crystal was illuminated with a Xenon arc lamp to observe the excitation spectrum for the one-phonon luminescence, no intrinsic luminescence but only the bound exciton luminescence was observed.[30] Detailed results and interpretation will be published elsewhere.

In summary, intrinsic indirect exciton recombination luminescence in tetragonal zinc diphosphide crystal is observed at various temperatures. One-phonon assisted luminescence consists of, at least, 30 components, reflecting the contribution of many momentum conserving phonons. Two-phonon assisted luminescence is confirmed, in which the contributing phonons are mainly the momentum conserving phonons taking part in the one-phonon exciton luminescence on the one hand and the phonons at the Γ point of the Brillouin zone on the other hand.

Acknowledgments

This work was partly supported by a Grant-in-Aid for Scientific Research from the Ministry of Education, Science and Culture.

1) I. J. Hegyi, E. E. Loebner, E. W. Poor Jr. and J. G. White: J. Phys. Chem. Solids **24** (1963) 333.
2) M. E. Fleet and T. A. Mowles: Acta. Crystallogr. Sect. C **40** (1984) 1778.
3) A. B. Pevtsov, S. A. Permogorov, A. V. Sel'kin, N. N. Syrbu and A. G. Umanets: Sov. Phys. Semicond. **16** (1982) 897.
4) O. Arimoto, S. Okamoto and K. Nakamura: J. Phys. Soc. Jpn. **59** (1990) 3490.
5) O. Arimoto, M. Tachiki and K. Nakamura: J. Phys. Soc. Jpn. **60** (1991) 4351.
6) S. Taguchi, T. Goto, M. Takeda and G. Kido: J. Phys. Soc. Jpn. **57** (1988) 3256.
7) T. Goto, S. Taguchi, Y. Nagamune, S. Takeyama and N. Miura: J. Phys. Soc. Jpn. **58** (1989) 3822.
8) T. Goto, S. Taguchi, K. Cho, Y. Nagamune, S. Takeyama and N. Miura: J. Phys. Soc. Jpn. **59** (1990) 773.
9) O. Arimoto, H. Takeuchi and K. Nakamura: Phys. Rev. B **46** (1992) 15512.
10) M. Sugisaki, M. Eguchi, O. Arimoto and K. Nakamura: J. Phys. Soc. Jpn. **62** (1993) 4533.
11) O. Arimoto, M. Sugisaki, K. Nakamura, K. Tanaka and T. Suemoto: J. Phys. Soc. Jpn. **63** (1994) 4249.
12) M. Sugisaki, M. Nishikawa, O. Arimoto, K. Nakamura, K. Tanaka and T. Suemoto: J. Phys. Soc. Jpn. **64** (1995) 3508.
13) D. Fröhlich, M. Schlierkamp, J. Schubert, S. Spitzer, O. Arimoto and K. Nakamura: Phys. Rev. B **49** (1994) 10337.
14) M. Rubenstein and P. J. Dean: J. Appl. Phys. **41** (1970) 1777.
15) I. S. Gorban', A. K. Tkachenko, I. I. Tychina and M. V. Chukichev: Sov. Phys. Semicond. **12** (1978) 1066.
16) I. S. Gorban', V. P. Grishchuk, L. S. Martsenyuk, A. V. Slobodyanyuk and Z. Z. Yanchuk: Sov. Phys. Semicond. **13** (1979) 1156.
17) V. V. Sobolev, A. I. Kozlov, Yu. I. Polygalov, V. E. Tupitsyn and A. S. Poplavnoi: Phys. Status Solidi B **154** (1989) 377.
18) N. N. Syrbu, V. I. Morozova and G. I. Stratan: Sov. Phys. Semicond. **23** (1989) 1096.
19) I. S. Gorban', V. A. Gorynya, V. I. Dugovoi and A. P. Makovetskaya: Sov. Phys. Solid State **17** (1975) 1070.
20) E. G. Kuz'minov, A. A. Andreev, E. M. Smolyarenko and A. U. Sheleg: Sov. Phys. Solid State **21** (1979) 1218.
21) A. V. Slobodyanyuk: Sov. Phys. Solid State **28** (1986) 1845.
22) N. N. Syrbu and V. E. L'vin: Sov. Phys. Semicond. **25** (1991) 1062.
23) N. N. Syrbu and V. E. L'vin: Sov. Phys. Semicond. **25** (1991) 686.
24) M. Yoshida, N. Ohno, K. Nakamura and Y. Nakai: Phys. Status Solidi B **109** (1982) 503.
25) R. J. Elliott: Phys. Rev. **108** (1957) 1384.
26) G. A. Thomas, M. Capizzi, W. Weber, E. I. Blount and M. Lax: Phys. Rev. Lett. **37** (1976) 1000.
27) P. J. Dean, E. C. Lightowlers and D. R. Wright: Phys. Rev. **140** (1965) A352.
28) P. J. Dean, J. R. Haynes and W. F. Flood: Phys. Rev. **161** (1967) 711.
29) N. O. Folland: Phys. Rev. B **1** (1970) 1648.
30) Y. Mizushima: private communication.